Mechanism and Machine Theory 134 (2019) 249–266

Contents lists available at ScienceDirect

Mechanism and Machine Theory

journal homepage: www.elsevier.com/locate/mechmachtheory

Adaptive torque tracking control during slip engagement of a dry clutch in vehicle powertrain

Jinrak Park[a], Seibum Choi[a,*], Jiwon Oh[b], Jeongsoo Eo[b]

[a] Mechanical Engineering, KAIST, Daejeon 34141, Republic of Korea
[b] Research and Development Division, Hyundai Motor Group, 150 Hyundaiyeonguso-ro, Namyang-eup, Hwaseong-si, Gyeonggi-do 18280, Republic of Korea

ARTICLE INFO

Article history:
Received 21 June 2018
Revised 22 November 2018
Accepted 29 December 2018
Available online 4 January 2019

Keywords:
Slip engagement control
Dry clutch control
Engine clutch control
Clutch friction coefficient
Clutch touch point

ABSTRACT

Dry clutches have been gaining its popularity for use in the transmission systems of small and medium-sized vehicles as well as the engine clutch systems of parallel hybrid vehicles. With this trend, the ability to appropriately control the amount of torque transferred through the dry clutch becomes important. This paper addresses a feedforward control method of clutch torque during slip engagement of a dry clutch utilizing a clutch friction model. In many studies, the clutch friction coefficient is considered as the only uncertain parameter in the clutch friction model. However, the clutch touch point can also serve as a major source of uncertainty in the clutch friction model. Thus, this paper proposes a simultaneous adaptation method to estimate the clutch friction coefficient and the clutch touch point in real time and a feedforward control method of clutch torque during slip engagement of a dry clutch based on the proposed adaptation algorithm. This control approach is applied to the slip engagement control of a dry engine clutch in a parallel hybrid vehicle and its effect is experimentally verified using a production vehicle.

1. Introduction

Clutch control in the vehicle powertrain has a significant effect on vehicle performance and ride comfort. Typical examples are transmission clutch control and engine clutch control for a parallel hybrid vehicle. When the clutch systems are controlled appropriately, the cutoff and vibration of driving torque, generated by an engine and a motor and transmitted to the wheel end, are minimized, and the running performance and ride comfort of a vehicle at the same time can thereby be improved [1–3].

There are two kinds of dry clutch engagement methods. The first is the synchronization engagement method in which a clutch is engaged after the speed of both sides of the clutch is synchronized. The second is the slip engagement method in which a clutch is engaged when the speed of both sides of the clutch is different. In the case of the synchronization engagement method, compared to the slip engagement, energy loss due to clutch friction is small, and little clutch wear and vibration of driving torque during clutch engagement occur. Thus, the synchronization method is mainly utilized for clutch engagement in production vehicles [4,5].

Fig. 1 shows a lumped inertia driveline model of a parallel hybrid vehicle. As shown in this figure, there are two clutches in the driveline of a parallel hybrid vehicle: a transmission clutch and an engine clutch [6]. In the case of the transmission

* Corresponding author.
E-mail addresses: pjr1413@kaist.ac.kr (J. Park), sbchoi@kaist.ac.kr (S. Choi), jwo@hyundai.com (J. Oh), fineejs@hyundai.com (J. Eo).

https://doi.org/10.1016/j.mechmachtheory.2018.12.033
0094-114X/

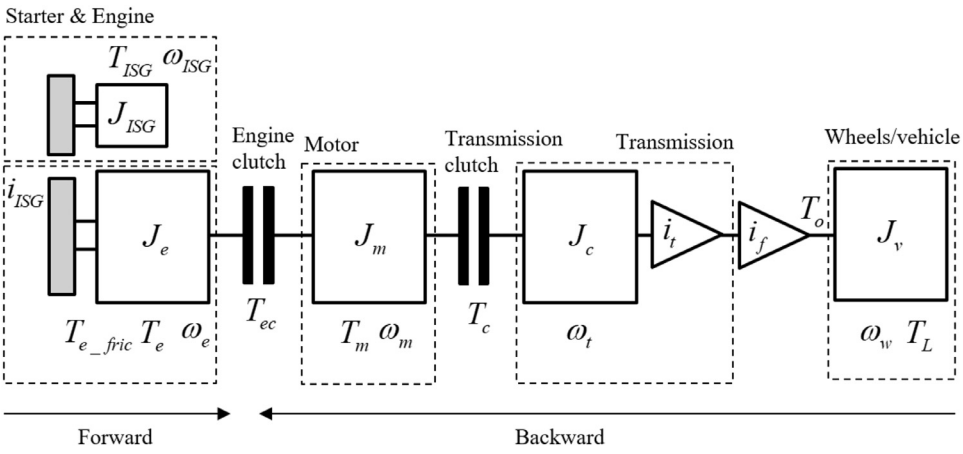

Fig. 1. Lumped inertia driveline model of a parallel hybrid vehicle.

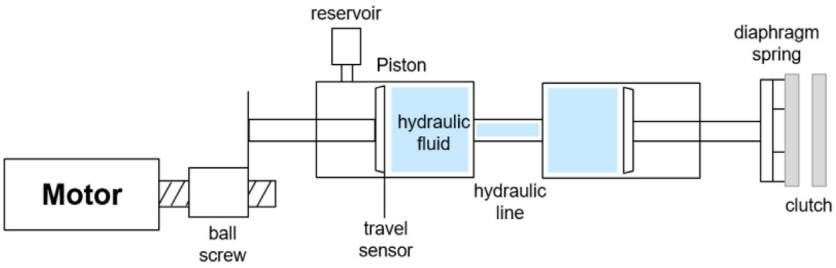

Fig. 2. Structure of the clutch actuator.

clutch, slip engagement is always required when gear shift occurs since the clutch should be engaged when the speed of the engine and the speed of the input shaft of the transmission are different.

Also, in the case of the engine clutch, slip engagement is required depending on situations. An Integrated Starter and Generator (ISG) is needed to synchronize the engine speed to the motor speed in an engine clutch system. However, considering a parallel hybrid system without an ISG, slip engagement is required since the engine clutch should be engaged when the speed of the engine and the speed of the motor are different. Also, in a parallel hybrid system, slip engagement is often required when the torque capacity of the driving motor is small; for example, when driving torque, which is greater than the torque capacity that the driving motor can manage, is needed on a steep hill, and the motor speed is lower than the engine idle speed. As such, there are situations where slip engagement is required in a transmission clutch or engine clutch system. On the other hand, when clutch slip engagement is performed, energy loss, clutch wear due to clutch friction, and driving torque vibration can occur, and hence precision clutch slip control is required to minimize these drawbacks.

On the other hand, during clutch slip engagement, since clutch torque is directly related to energy loss, clutch wear, and vibration of driving torque, preferably the clutch slip control is mainly performed using the clutch torque as a control variable. However, torque sensors that measure the clutch torque are expensive and bulky, and hence cannot be installed in a real vehicle. Therefore, the clutch torque should be considered to be unmeasurable. The clutch slip control should thus be performed using the clutch slip speed as a control variable [7,8], or a clutch torque estimator should be designed to use the clutch torque as a control variable [4,5,9]. On the other hand, since a torque estimator always includes torque error, it would not be desirable to perform feedback torque tracking control using the estimated torque directly [10]. Thus, many studies have proposed a feedforward torque tracking controller using a clutch friction model [11–14].

Fig. 2 shows the structure of the clutch actuator that was utilized in this study. As shown in Fig. 2, a clutch friction model can represent the relationship between the hydraulic line pressure and the clutch torque in a clutch actuator system with a hydraulic line or the relationship between a position variable (for example, the piston position) and the clutch torque. In this study, since the piston position was measurable in the clutch actuator system, the clutch friction model was regarded as the relationship between the piston position and the clutch torque.

However, there are uncertain parameters in the clutch friction model that vary in real time such as the clutch friction coefficient and the clutch touch point. Thus, the clutch friction model should be corrected utilizing a clutch torque estimator. The clutch friction coefficient can be changed depending on the variation of the temperature and surface roughness of the clutch plates. Thus, previous studies have mainly focused on the adaptation of the clutch friction coefficient in the clutch friction model [7,8,12,15]. However, as shown in Fig. 2, when there is a hydraulic line in a clutch actuator system, the clutch

touch point can be changed due to contraction and expansion of the fluid in the hydraulic line depending on the fluid temperature. In addition, the clutch touch point can be changed if the fluid slightly leaks from the hydraulic line, and also can be changed by clutch wear. For these reasons, the adaptation of the clutch touch point can be as important as that of the clutch friction coefficient [16].

In previous studies, the clutch touch point is estimated in a special mode only, not in real time [17,18]. For example, the hydraulic pressure is memorized when the driveline speed is changed while the transmission clutch is being engaged slightly in engine idle, vehicle stop, and transmission neutral state, and it is then filtered to estimate the clutch touch point. In this case, the driver can feel strange to the special action. Also, the clutch slip control cannot cope with the real time variation of the clutch touch point, and the torque tracking performance thus can become worse. In addition, when the clutch touch point is estimated in real time, it is possible to diagnose the fault of the actuator hydraulic line by observing the change of the touch point.

This paper presents a feedforward control method of clutch torque during slip engagement of a dry clutch in the vehicle powertrain based on the adaptation of the clutch friction model, where the uncertain parameters are the clutch friction coefficient and the clutch touch point. The adaptation of the two uncertain parameters is conducted at the same time, the target piston position is calculated using the inverse function of the compensated clutch friction model, and the piston position is feedback controlled using the piston position sensor. The algorithm proposed in this paper was verified through experiments using a production vehicle, by applying the algorithm to slip engagement control of a dry engine clutch located between the engine and the motor of a parallel hybrid vehicle. It can also be used for slip engagement control of a dry clutch of transmissions such as automatic transmissions, automatic manual transmissions, and dual clutch transmissions.

The main contribution of this study is the proposal of a simultaneous adaptation method of the clutch friction coefficient and the clutch touch point in real time using the estimated clutch torque, and a feedforward control method of clutch torque during slip engagement of a dry clutch based on the corrected friction model using the estimated clutch friction coefficient and touch point.

This paper is organized as follows: Section 2 explains the method to estimate the engine clutch torque. Section 3 deals with the adaptation method of the clutch friction model, as well as the feedforward control method of the target clutch. Section 4 shows the experimental results of the proposed algorithm. Finally, Section 5 concludes this paper.

2. Engine clutch torque estimation

2.1. Driveline model of a parallel hybrid vehicle

First, to perform torque-based slip engagement control of an engine clutch, the engine clutch torque must be estimated. This is because, as noted in the introduction section, there is no torque sensor in a commercial vehicle that can measure the engine clutch torque.

Referring to Fig. 1, a parallel hybrid vehicle can be modeled as a lumped inertia model as follows [19–21].

$$J_e\dot{\omega}_e = T_e - T_{ec} \tag{1}$$

$$J_m\dot{\omega}_m = T_{ec} + T_m - T_c \tag{2}$$

$$J_c\dot{\omega}_c = T_c - \frac{1}{i_t i_f}T_o \tag{3}$$

$$J_v\dot{\omega}_w = T_o - T_L \tag{4}$$

$$T_o = k_o\left(\frac{\theta_c}{i_t i_f} - \theta_w\right) + b_o\left(\frac{\omega_c}{i_t i_f} - \omega_w\right) \tag{5}$$

$$T_L = r_w\{m_v g\sin(\Phi_{road}) + K_{rr}m_v g\cos(\Phi_{road}) + \frac{1}{2}\rho v_x^2 C_d A\} \tag{6}$$

where T_e, T_{ec}, T_m, T_c, T_o and T_L represent the engine, engine clutch, motor, transmission clutch, output shaft, and driving resistance torque, respectively, and ω_e, ω_m, ω_c and ω_w indicate the rotational speed of the engine, motor, transmission input shaft, and wheel, respectively, and i_t, i_f, k_o, b_o, r_w, m_v, g, Φ_{road}, K_{rr}, ρ, v_x, C_d and A denote the transmission gear ratio, final gear ratio, spring constant of the output shaft, damping constant of the output shaft, wheel radius, vehicle mass, gravitational acceleration, tire rolling resistance coefficient, air density, vehicle longitudinal velocity, aerodynamic drag coefficient, and frontal area of a vehicle, respectively.

As shown in Fig. 1, in a parallel hybrid vehicle, there are two ways of estimating the engine clutch torque: the forward direction from the engine torque or the backward direction from the output shaft torque. In many studies, Eqs. (5) and (6) have been actively utilized when estimating the driveline clutch torque in the backward direction of the driveline.

Eq. (5) is a torque compliance model expressing the twist of a shaft, and Eq. (6) is a model expressing the driving resistance of a vehicle.

On the other hand, when utilizing Eq. (5) for estimation of the driveline clutch torque, the speed of the driveline shafts must be integrated to calculate the angle of the shafts since the speed of the shafts is measured rather than the angle in a production vehicle. Thus, backlash between shaft joints can affect the performance of clutch torque estimation considerably since the direction of shaft rotation is changed frequently during clutch engagement, and noise in the speed of the shafts can affect the performance as well [22,23]. Also, when utilizing Eq. (6) for estimating the driveline clutch torque, estimation of the vehicle mass and road grade may be newly required since clutch slip engagement often occurs on a ramp.

Therefore, in this study, an engine clutch torque estimator based on the engine torque in the forward direction of the driveline was utilized actively to reduce the computational complexity of the torque estimation algorithm and improve practicality in various environments. The following subsection introduces the forward path estimator of the engine clutch torque, which is used to adapt the clutch friction model later.

2.2. Forward path estimator of engine clutch torque

In this subsection, the forward path estimator of engine clutch torque used in this study and some comparative estimators that use both the forward and backward path methods are introduced to explain the necessity of the forward path estimator and the estimation results of each estimator will be discussed in the later results section. Before showing the forward path estimator, comparative estimators are first described.

The first comparative engine clutch torque estimator is a modified version of the model reference PI estimator presented in previous studies [19,20] Equations of the estimator are written in the appendix for the sake of brevity. The model reference PI estimator utilizes all of the model Eqs. (1)–(6) mentioned in the previous subsection. A measurement update term is added to the output shaft torque model in the modified version compared with the original version since the uncertainty of the output shaft torque model was large, and the output shaft torque diverged in some situations in application to a real vehicle. The details will be discussed in the later results section.

In addition, a Kalman filter based engine clutch torque estimator is newly designed as the second comparative estimator using the driveline lumped inertia model of Eqs. (1)–(3) and the output shaft torque compliance model of Eq. (5). As described in the previous subsection, since the angle of the driveline shafts cannot be measured in a real vehicle, Eq. (5) should be modified, and thus it is differentiated as follows and the damping coefficient is assumed to be 0.

$$\dot{T}_o = k_o\left(\frac{\omega_c}{i_t i_f} - \omega_w\right) \tag{7}$$

The driveline dynamics can then be described using Eqs. (1)–(4) and (7) as follows.

$$\begin{aligned}
&\dot{\mathbf{X}} = \mathbf{AX} + \mathbf{BU}\\
&\mathbf{Y} = \mathbf{CX}\\
&\mathbf{X} = \begin{pmatrix}\omega_e & \omega_m & \omega_c & \omega_w & T_{ec} & T_c & T_o & T_L\end{pmatrix}^T\\
&\mathbf{U} = \begin{pmatrix}T_e & T_m\end{pmatrix}^T\\
&\mathbf{A} = \begin{pmatrix}
0 & 0 & 0 & 0 & -1/J_e & 0 & 0 & 0\\
0 & 0 & 0 & 0 & 1/J_m & -1/J_m & 0 & 0\\
0 & 0 & 0 & 0 & 0 & 1/J_c & -1/i_t i_f J_c & 0\\
0 & 0 & 0 & 0 & 0 & 0 & 1/J_v & -1/J_v\\
0 & 0 & 0 & 0 & 0 & 0 & 0 & 0\\
0 & 0 & 0 & 0 & 0 & 0 & 0 & 0\\
0 & 0 & k_o/i_t i_f & -k_o & 0 & 0 & 0 & 0\\
0 & 0 & 0 & 0 & 0 & 0 & 0 & 0
\end{pmatrix}\\
&\mathbf{B} = \begin{pmatrix}0 & 1/J_m & 0 & 0 & 0 & 0 & 0 & 0\\ 1/J_e & 0 & 0 & 0 & 0 & 0 & 0 & 0\end{pmatrix}^T,\quad \mathbf{C} = \begin{pmatrix}1 & 0 & 0 & 0 & 0 & 0 & 0 & 0\\ 0 & 1 & 0 & 0 & 0 & 0 & 0 & 0\\ 0 & 0 & 1 & 0 & 0 & 0 & 0 & 0\\ 0 & 0 & 0 & 1 & 0 & 0 & 0 & 0\end{pmatrix}^T
\end{aligned} \tag{8}$$

A discrete Kalman filter is subsequently designed by discretizing the above continuous system. Equations of the discrete Kalman filter are written in the appendix for the sake of brevity.

On the other hand, the computation burden of the model reference PI estimator and the Kalman filter based estimator, which are comparative estimators, is large since the estimators have a number of states. Furthermore, the output shaft torque model expressed as Eq. (5) and the driving resistance torque expressed as Eq. (6) were quite different from the actual model in a real vehicle application. Hence, when estimating the output shaft torque and the driving resistance torque, the proportion of the measurement update was much larger than the proportion of the model in the estimator. This means that the output shaft torque model and driving resistance torque model do not contribute significantly to accuracy improvement of the engine clutch torque estimation since it has large uncertainty in real vehicle application.

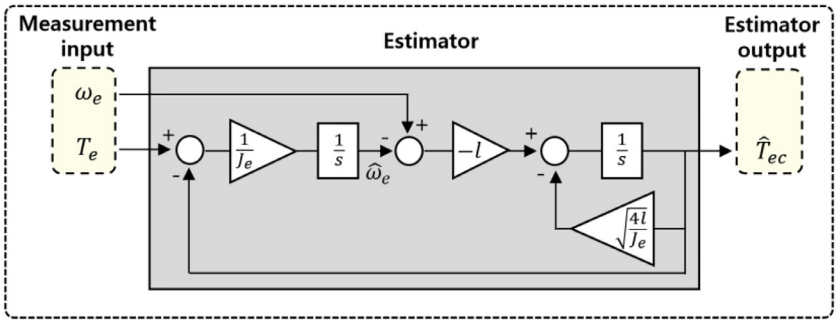

Fig. 3. Block diagram of the engine clutch estimator.

Therefore, in this paper, an engine clutch torque estimator in the forward direction of the driveline using only Eq. (1) is designed in order to reduce the computational complexity and reduce the effect of model uncertainty. In a previous study [21], a clutch torque estimator in the forward direction was designed as follows.

$$\dot{\hat{\omega}}_e = \frac{1}{J_e}(T_e - \hat{T}_{ec}) + l_1(\omega_e - \hat{\omega}_e) \tag{9}$$

$$\dot{\hat{T}}_{ec} = -l_2(\omega_e - \hat{\omega}_e) \tag{10}$$

where the symbol $\wedge$ represents an estimation variable, and l_1 and l_2 are tuning parameters.

Also, the differential equation of the engine clutch torque is expressed as follows, combining the above two equations.

$$\frac{J_e}{l_2}\ddot{\hat{T}}_{ec} + \frac{J_e l_1}{l_2}\dot{\hat{T}}_{ec} + \hat{T}_{ec} = T_e - J_e\dot{\omega}_e \tag{11}$$

Here, the estimated value of the engine clutch torque is a value obtained by passing the right term of the above equation through a second-order low-pass filter. Generally, when estimating the engine clutch torque using Eq. (1), the estimated value of the engine clutch torque is a value obtained by low-pass filtering the right term of the above equation. However, as seen in filtering Eq. (11) for the engine clutch torque estimator to the forward path proposed in the previous study, the estimator has two tuning parameters to adjust the cut-off frequency of the engine clutch torque filter.

In this study, a forward path engine clutch torque estimator with only one tuning parameter is designed and utilized for the later clutch friction model adaptation and the torque tracking control by modifying the above estimator with two tuning parameters.

$$\dot{\hat{\omega}}_e = \frac{1}{J_e}(T_e - \hat{T}_{ec}) \tag{12}$$

$$\dot{\hat{T}}_{ec} + 2\sqrt{\frac{l}{J_e}}\hat{T}_{ec} = -l(\omega_e - \hat{\omega}_e) \tag{13}$$

where l is a tuning parameter.

By combining the above two equations, the following differential equation of the engine clutch torque can be obtained.

$$\frac{J_e}{l}\ddot{\hat{T}}_{ec} + 2\sqrt{\frac{J_e}{l}}\dot{\hat{T}}_{ec} + \hat{T}_{ec} = T_e - J_e\dot{\omega}_e \tag{14}$$

As seen in the above equation, it is possible to adjust the cutoff frequency of the engine clutch torque filter by one tuning parameter. In addition, the above estimator does not require matrix computation, and thus the computational burden is very small. Also, there was no significant difference in performance compared with the comparative estimators although the equations of the estimator are very simple. A block diagram of the final forward path estimator is shown in Fig. 3.

The performance of the model reference PI estimator, the Kalman filter based estimator, and the forward path estimator will be compared in the later results section.

3. Clutch friction model adaptation and torque tracking control

3.1. Adaptation of the clutch touch point

Referring to Fig. 2, in this study, the clutch friction model represents the relationship between the piston position in the clutch actuator system and clutch torque since the piston position was measurable. This is described in the introduction section in detail.

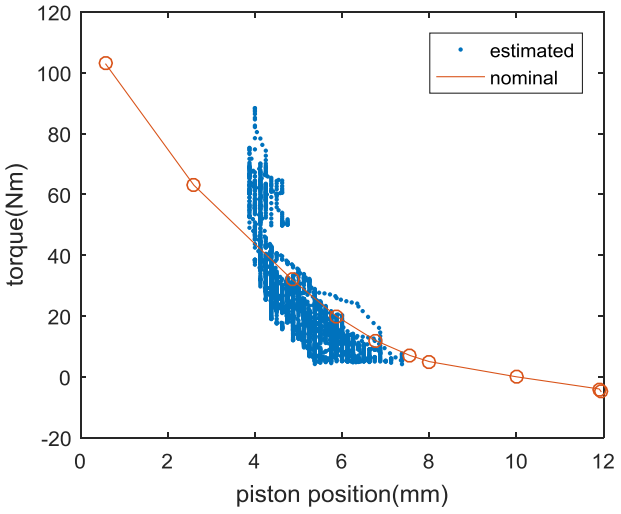

Fig. 4. Estimated piston position–engine clutch torque data.

In the previous section, the engine clutch torque was estimated. Therefore, the estimated clutch torque corresponding to the piston position can now be known for the period of clutch slip engagement and this information can be used to adapt the clutch friction model.

In the x-y coordinate system, where the x-axis and y-axis represent the piston position and the clutch torque, respectively, coordinate points are referred to as torque-stroke (T-S) data; the relationship curve of the piston position and clutch torque is referred to as a T-S curve. Fig. 4 shows the estimated T-S data and the nominal T-S curve. The estimated engine clutch torque mentioned in the previous section was utilized for the estimated T-S data. The nominal T-S curve was obtained experimentally, and utilized as the clutch friction model in this study.

The estimated engine clutch torque was extracted when the clutch torque was larger than 5 Nm, the clutch slip speed was greater than 20 rad/s, and the piston position was between 3 mm and 7.5 mm. The engine clutch considered in this paper is the normally closed type, and the piston is moving from 0 to 13.5 mm, and the engine clutch is fully closed and the clutch torque is maximal when the piston position is 0 mm.

As mentioned in the introduction section, there can be two uncertain parameters in a clutch friction model. The first is the clutch friction coefficient and the second is the clutch touch point. A clutch friction model can be expressed generally as follows.

$$T_{cl} = \mu_{cl} R_{cl} F(d, \lambda_{touch}) \tag{15}$$

where T_{cl}, μ_{cl}, R_{cl}, F, d and λ_{touch} represent the clutch torque, clutch friction coefficient, clutch radius, clutch normal force, actuator piston position, and clutch touch point, respectively.

In the clutch friction model, the clutch touch point refers to the piston position when the clutch starts transmitting torque. Also, the clutch normal force is a function of the piston position and the clutch touch point, which is characteristic of a clutch diaphragm spring.

Basically, the shape of a T-S curve is the same as that of a diaphragm spring characteristics curve (piston position-clutch normal force) since the T-S curve is a weighted function of the diaphragm spring characteristics curve. Thus, as shown in Eq. (15), assuming that the shape of the diaphragm characteristics curve and the effective radius of the clutch torque do not change, the variation of the clutch friction coefficient can affect the slope variation of the T-S curve, and the variation of the clutch touch point can affect the variation of the amount of parallel drifting of the T-S curve in the piston position axis.

Therefore, in this study, the estimation problem of the clutch friction coefficient and the clutch touch point is regarded as the same problem as the estimation of a multiplicative constant of the slope and the amount of parallel drifting in the piston position axis of a nominal T-S curve as follows.

$$T_{cl.r} = \mu_{cl.r} R_{cl} F(d, \lambda_{touch.r}) \tag{16}$$

$$\mu_{cl.r} = \hat{\alpha}_{cl} \mu_{cl.n} \tag{17}$$

$$\lambda_{touch.r} = \lambda_{touch.n} + \hat{\beta}_{cl} \tag{18}$$

where $T_{cl.r}$, α_{cl}, β_{cl}, $\mu_{cl.r}$, $\mu_{cl.n}$, $\lambda_{touch.r}$ and $\lambda_{touch.n}$ represent the actual clutch torque, multiplicative constant of the slope of a nominal T-S curve, the amount of parallel drifting in the piston position axis of a nominal T-S curve, actual clutch friction coefficient, nominal clutch friction coefficient, actual clutch touch point, and nominal clutch touch point, respectively.

That is, it is considered that the actual friction coefficient can be known if the multiplicative constant of the slope of the nominal T-S curve is known. Also, it is considered that the actual touch point can be known if the amount of parallel drifting in the piston position axis of a nominal T-S curve is known.

In this study, an adaptive feedforward control method of clutch torque during slip engagement of a dry clutch is proposed using the compensated T-S curve, as given in Eq. (16). A nominal T-S curve is compensated using a multiplicative constant of the slope and the amount of parallel drifting in the piston position axis of the nominal T-S curve, as shown in Eqs. (16)–(18). Hereafter, the multiplicative constant of the slope of the nominal T-S curve is called the friction coefficient gain.

There are two possible ways to estimate the friction coefficient gain and the amount of parallel drifting. The first is to estimate the two parameters, assuming that the variation of the amount of parallel drifting is affected by the variation of the friction coefficient gain. For example, referring to Fig. 4, a recursive least square method can be used to estimate the friction coefficient gain and the amount of parallel drifting so that the shape of the nominal T-S curve matches the shape of the estimated T-S data as closely as possible. In this case, the friction coefficient gain is abruptly changed when there is an error in the estimated engine clutch torque, and the amount of parallel drifting is also changed accordingly, and then the shape of the compensated T-S curve is changed suddenly. Therefore, the feeling of torque transmission through the clutch during slip engagement can be changed suddenly if the feedforward torque tracking control using the compensated T-S curve is performed.

The second is to estimate the two parameters, assuming that the variation of the amount of parallel drifting is not affected by the variation of the friction coefficient gain. In this case, even if the friction coefficient gain is changed greatly, this change does not affect the change in the amount of the parallel drifting, and thus the feeling of torque transmission through the clutch is not altered rapidly. Therefore, it is possible to perform robust control against the clutch torque error. Thus, in this study, the amount of parallel drifting of the nominal T-S curve is first estimated and the friction coefficient gain of the model is then estimated using the amount of parallel drifting.

First, to estimate the amount of parallel drifting, the clutch touch point is estimated by calculating the moving averaged value of the measured piston position (called the first step touch point), where the corresponding estimated clutch torque is within the specific threshold, during clutch slip engagement, as given below. In this paper, the lower and upper thresholds were set as 5 and 10 Nm.

$$l_3 < \hat{T}_{ec} < l_4 \tag{19}$$

$$\hat{\delta}_{k+1} = \frac{n}{n+1}\hat{\delta}_k + \frac{1}{n+1}d_{k+1} \tag{20}$$

where l_3, and l_4 are the lower, and upper thresholds of the estimated engine clutch torque, and d and δ indicate the actuator piston position, and the first step touch point of the engine clutch, and the subscript k denotes the time step during engine clutch slip engagement.

The adaptation of the final clutch touch point (called the second step touch point) is then conducted using the first step touch point additionally whenever the clutch slip engagement is finished since the touch point is a slowly varying variable.

$$\Delta\hat{\lambda}_{i+1} = \gamma_\lambda(\hat{\delta}_i - \hat{\lambda}_i), \quad \gamma_\lambda > 0 \tag{21}$$

$$\hat{\lambda}_{i+1} = \hat{\lambda}_i + \Delta\hat{\lambda}_{i+1} \tag{22}$$

where Δ represents the amount of variation, and λ and γ_λ denote the second step touch point of the engine clutch and an update gain of the second step touch point, and the subscript i denotes the number of engine clutch engagements.

A fast-varying first step touch point can be used to diagnose the hydraulic line failure, as noted in the introduction section, and a slowly-varying second step touch point can be used for clutch slip control.

Finally, the amount of parallel drifting of the friction model in the piston position axis (x-axis in Fig. 4) is calculated using the second step touch point, as given below. It is utilized to estimate the clutch friction coefficient gain and to control the slipping clutch.

$$\hat{\beta} = \hat{\lambda} - \lambda_n \tag{23}$$

where λ_n and β represent the nominal engine clutch touch point and the amount of parallel drifting of the nominal engine clutch T-S curve in the piston position axis.

3.2. Adaptation of the clutch friction coefficient

In this subsection, the friction coefficient gain is estimated using the amount of parallel drifting of the clutch friction model, which is estimated in the previous subsection. As in Eq. (16), the engine clutch torque is defined using a multiplicative constant (called a friction coefficient gain), and the amount of parallel drifting of the clutch friction model, and the update error of the friction coefficient gain is defined as follows [24–26].

$$T_{ec} = \alpha T_{ec.n}(d - \hat{\beta}), \quad T_{ec.n}(d - \hat{\beta}) > 0 \tag{24}$$

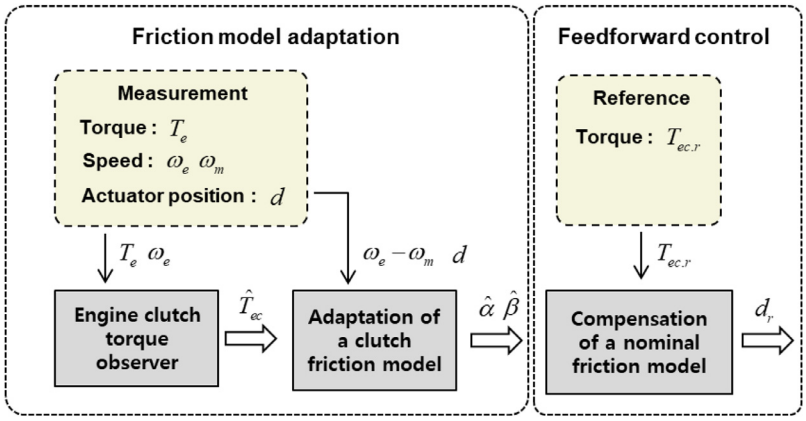

Fig. 5. Structure of the adaptive feedforward control algorithm of a dry engine clutch.

$$\varepsilon = \hat{T}_{ec} - T_{ec} = (\hat{\alpha} - \alpha)T_{ec.n}(d - \hat{\beta}) = \tilde{\alpha}T_{ec.n}(d - \hat{\beta}) \tag{25}$$

where $T_{ec.n}$, $\alpha, \tilde{\alpha}$ and ε indicate the nominal engine clutch torque, the friction coefficient gain of the engine clutch, the error of the friction coefficient gain between the estimated and actual values, and the update error of the friction coefficient gain, respectively.

The adaptation law of the friction coefficient gain is then defined as follows.

$$\dot{\hat{\alpha}} = -\gamma_\alpha \varepsilon, \quad \gamma_\alpha > 0 \tag{26}$$

where γ_α is an adaptation gain of the friction coefficient gain.

The estimated clutch friction coefficient can then be calculated as given below.

$$\hat{\mu} = \hat{\alpha}\mu_n \tag{27}$$

where μ and μ_n denote the engine clutch friction coefficient and the nominal engine clutch friction coefficient.

For the stability proof of the adaptation law of the friction coefficient gain, the error dynamics of the friction coefficient gain is defined as follows.

$$\tilde{\alpha} = \hat{\alpha} - \alpha \tag{28}$$

$$\dot{\tilde{\alpha}} = -\gamma_\alpha \tilde{\alpha} T_{ec.n}(d - \hat{\beta}) \tag{29}$$

The stability is then proved using a simple Lyapunov candidate as given below.

$$V = \frac{1}{2\gamma_\alpha}\tilde{\alpha}^2 > 0 \tag{30}$$

$$\dot{V} = -\tilde{\alpha}^2 T_{ec.n}(d - \hat{\beta}) < 0 \tag{31}$$

3.3. Feedforward controller

In this subsection, the slip engagement feedforward controller of a dry clutch is designed using the estimated friction coefficient gain and the amount of parallel drifting of the clutch friction model. Referring to Eq. (24), the inverse of Eq. (24) can be expressed as follows.

$$d = \alpha {T_{ec.n}}^{-1}(T_{ec}) + \hat{\beta} \tag{32}$$

The reference piston position then can be calculated according to the reference engine clutch torque using the estimated friction coefficient gain as follows.

$$d_r = \hat{\alpha} {f_n}^{-1}(T_{ec.r}) + \hat{\beta} \tag{33}$$

where d_r and $T_{ec.r}$ represent the reference actuator piston position and the reference engine clutch torque.

The feedback control of the piston position is then performed using the piston position sensor based on a PID controller. The details of the piston position feedback control using the PID controller are omitted because it is simple.

Finally, the structure of the adaptive feedforward control algorithm of a dry engine clutch proposed in this study can be depicted as shown in Fig. 5.

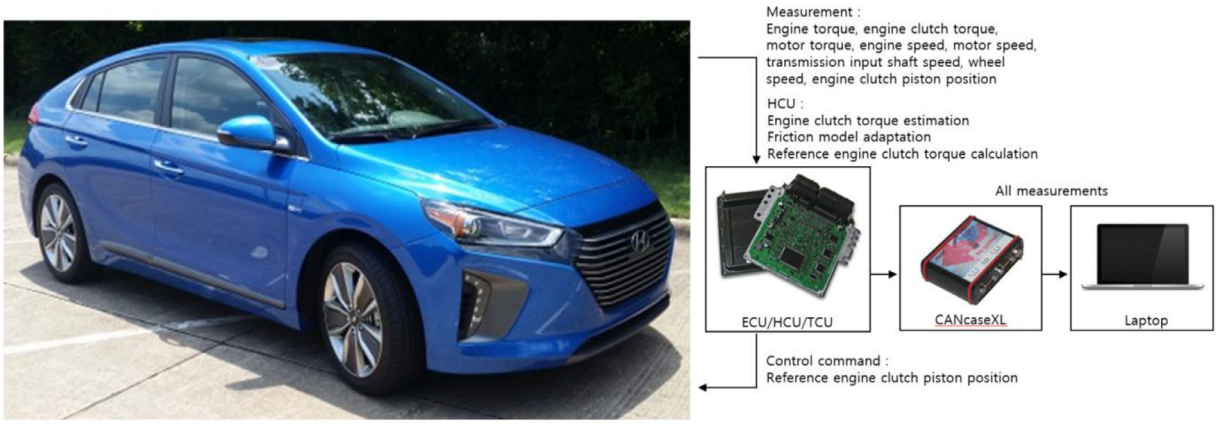

Fig. 6. Experimental production vehicle and data flow diagram.

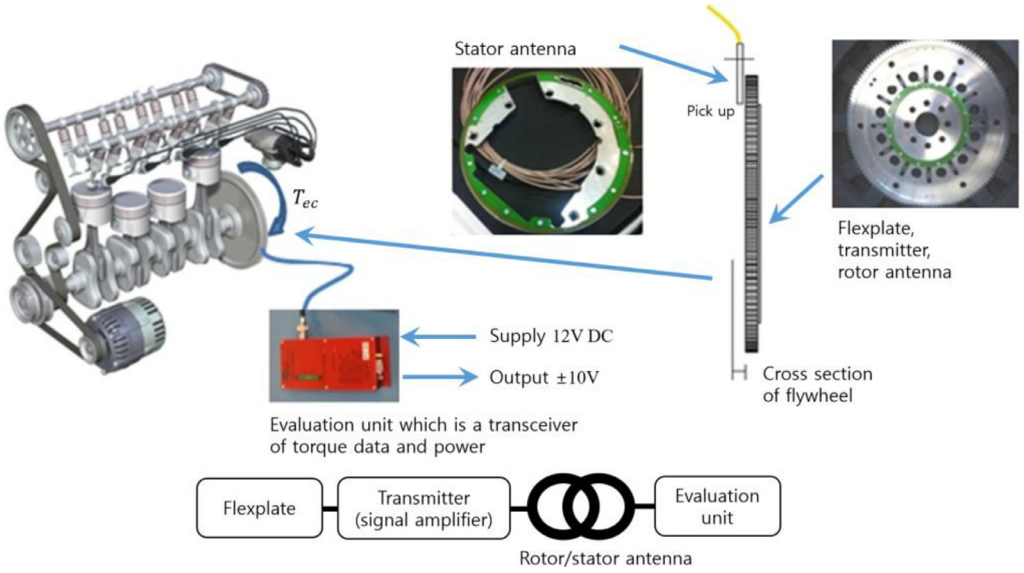

Fig. 7. Installation diagram of the clutch torque sensor.

4. Experimental results

4.1. Engine clutch torque estimation

In this subsection, the performance of the engine clutch torque estimator proposed in this paper was verified through an experiment with a production parallel hybrid vehicle. Fig. 6 shows the experimental production vehicle and data flow diagram. A schematic diagram of the experimental vehicle driveline is presented in Fig. 1. The experimental vehicle was equipped with a dual clutch transmission (DCT). Since gear shift does not occur during slip engagement of the engine clutch, only one transmission shaft is shown in Fig. 1.

Fig. 7 shows the installation diagram of the clutch torque sensor. A wireless flexplate torque sensor from the HBM Company was attached to the engine flywheel to measure the engine clutch torque and all parts including the ECU, TCU, and Hybrid Control Unit (HCU) except for the modification of the experimental vehicle for the torque sensor were original. The control algorithm was programmed in the control units, and measurements and command signals were logged by a laptop through CANcaseXL.

Here, the engine torque used as an input variable of the engine clutch estimators, which were introduced in Section 2, can be obtained in a real vehicle application as the sum of the indicated engine torque, which is generated by the fuel combustion, the friction torque, and the starter and generator torque. The indicated engine torque and the friction torque can be obtained as a function of the engine speed, intake manifold pressure, numbers that describe whether accessories are working, and some other parameters. Also, the starter and generator torque can be obtained through current measurement

Table 1
Model parameters.

Engine inertia, kg m^2	$J_e = 0.14$
Motor inertia, kg m^2	$J_m = 0.1$
Clutch inertia, kg m^2	$J_c = 0.1$
Vehicle inertia, kg m^2	$J_v = 142.07$
Output shaft torsional stiffness, N m	$k_o = 700$
Output shaft torsional damping coefficient, kg m^2/s	$b_o = 1300$
Transmission 1st gear ratio*final gear ratio, -	$i_{t.1}i_f = 16.1924$
Transmission 2nd gear ratio*final gear ratio, -	$i_{t.2}i_f = 9.2852$
Vehicle mass, kg	$m_v = 1500$
Wheel radius, m	$r_w = 0.3076$
Air density, kg/m^3	$\rho = 1.226$
Aerodynamic drag coefficient, -	$C_d = 0.3$
Effective frontal area, m^2	$A = 1$
Tire rolling resistance coefficient, -	$K_{rr} = 0.01$

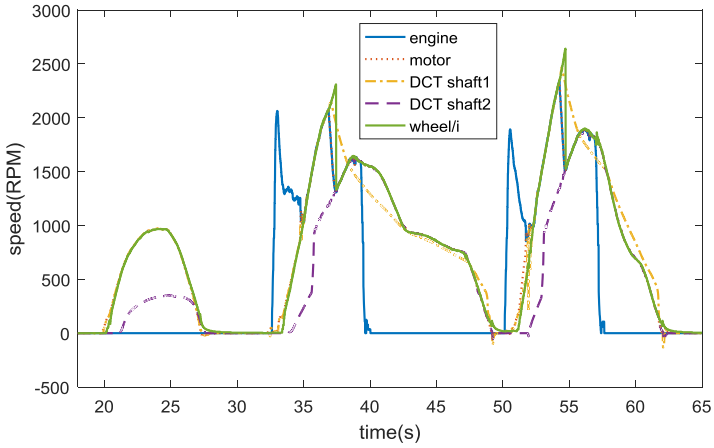

Fig. 8. Driveline speed during the verification experiment of the engine clutch torque estimator.

of the starter and generator. The details of the engine torque estimation are not addressed here since it deviates somewhat from the scope of this paper. However, the engine torque was assumed to be a measurable variable in this study.

In addition, the driving motor torque could be obtained through current measurement of the driving motor, and the engine speed, motor speed, two input shafts' speed of a dual clutch transmission, and wheel speed were measurable in the experimental vehicle.

During the first experiment, the engine clutch was slipping and engaged two times while the car launched. The model parameters used in this paper are shown in Table 1.

Figs. 8 and 9 show the driveline speed and torque during the experiment. In the legend, DCT shaft1 and DCT shaft2 denote the input shaft speed of the odd gear stage and even gear stage in the dual clutch transmission of the experimental vehicle, respectively. Also, is the gear ratio from the input shaft of an engaged gear to the wheel.

Figs. 10 and 11 show the results of the engine clutch torque estimation during the experiment. Fig. 11 is an enlarged graph of Fig. 10 for a certain period. In Figs. 10 and 11, the estimated engine clutch torque by the forward path estimator, model reference PI estimator, and Kalman filter based estimator was compared with the measured value. In the legend, forward path, model reference, and Kalman denote the estimated engine clutch torque by the forward path estimator, the model reference PI estimator, and the Kalman filter based estimator, respectively. Also, 'measured' denotes the measured engine clutch torque and 'slipping phase' means the period when the clutch slip speed is larger than 20 rad/s, the piston position is between 0 and 13.5 mm, and the engine clutch is slipping and being engaged.

Fig. 14 shows the estimated T-S curve data during the slipping phase of the engine clutch. In Fig. 14, it can be seen that the estimated engine clutch torque by the Kalman filter-based estimator, the forward path estimator, and the model-based PI estimator was in turn closer to the measured engine clutch torque during the slipping phase. Table 2 shows the RMS error between the estimated and measured engine clutch torque during the slipping phase depending on each method. Similar to the results shown in Fig. 14, the RMS error between the estimated and measured value was small in the order of the Kalman filter based estimator, the forward path estimator, and the model reference PI estimator. However, the differences among the RMS error of each method were small. This reflects that the effect of the torque estimation in the backward direction of the driveline in the entire torque estimation process is small.

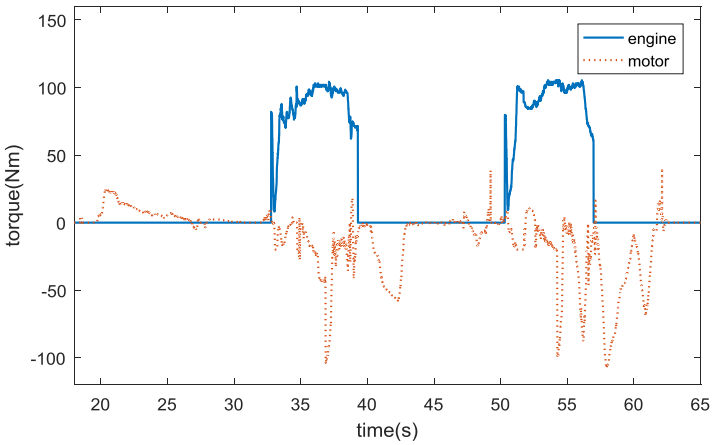

Fig. 9. Driveline torque during the verification experiment of the engine clutch torque estimator.

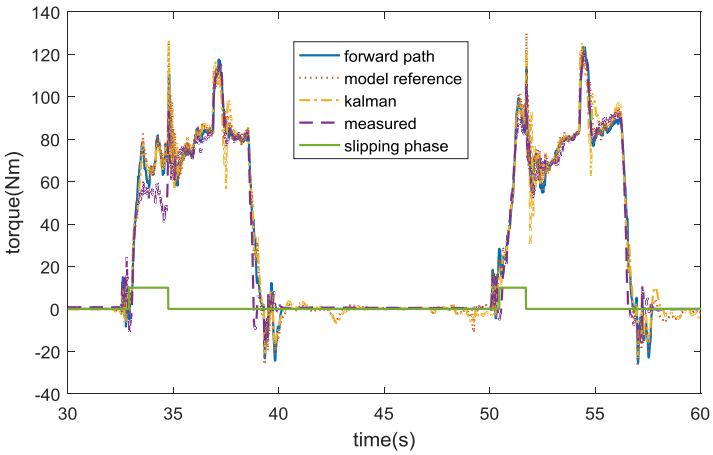

Fig. 10. Estimated engine clutch torque during the verification experiment of the engine clutch torque estimator.

Table 2
RMS error between the estimated and measured clutch torque during slipping phase.

Method	RMS error (Nm)
Forward path estimator	13.35
Model reference PI estimator	14.46
Kalman filter	12.79

Fig. 12 shows the output shaft torques calculated by the following three methods. The first method is to calculate the output shaft torque using the measured engine clutch torque and the lumped inertia model, which are expressed as Eqs. (2) and (3), and the second method is to calculate the output shaft torque using the shaft torque compliance model, which is expressed as Eq. (5), and the third method is to calculate the output shaft torque using the driving resistance torque model and the lumped inertia model, which are expressed as Eqs. (4) and (6). Measured values of motor torque and driveline speed were utilized in the calculation process.

The output shaft torque obtained by the first method is regarded as the actual value and compared with the output shaft torque obtained by the other two methods. It then can be seen in Fig. 12 that there are considerable difference between the output shaft torque obtained by the shaft compliance model and the driving resistance torque model, and the actual output shaft torque. Also, it can be seen that the output shaft torque obtained by the shaft torque compliance model is divergent in several sections. This is due to the influence of backlash between the shaft joints at around 20 s and the uncertainty of the gear ratio during transmission gear shift at around 37 s, 50 s, 55 s, and 62 s. Furthermore, the output shaft torque obtained by the driving resistance torque model showed a pure time delay compared with the actual value when the output shaft torque suddenly increased at around 33 s and 52 s.

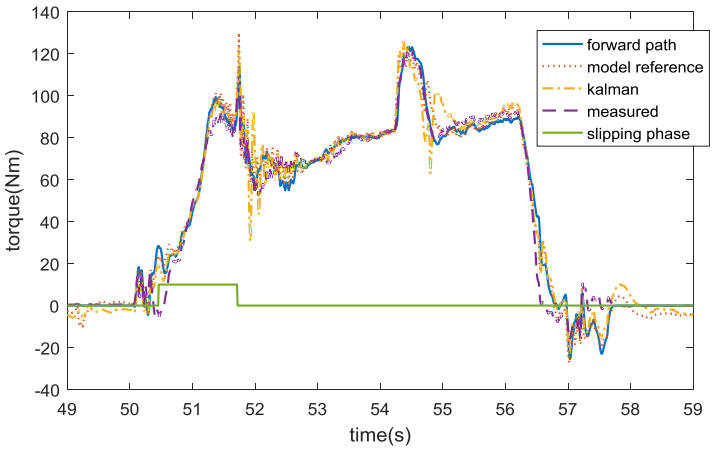

Fig. 11. Enlarged graph of estimated engine clutch torque during the verification experiment of the engine clutch torque estimator.

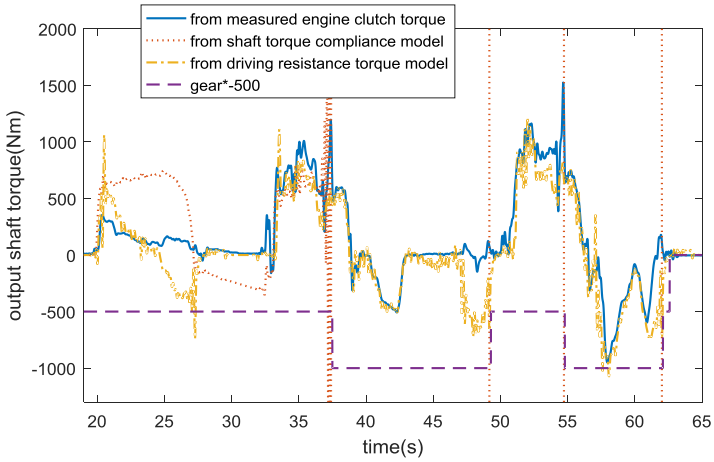

Fig. 12. Comparison of output shaft torque depending on a model.

From this result, it can be found that the shaft torque compliance model and the driving resistance torque model are significantly different from the actual model in real vehicle application. This means that the proportion of the measurement update should be much larger than the proportion of the model when estimating the output shaft torque and driving resistance torque. In addition, the output shaft torque model and the driving resistance torque model cannot play a significant role in improving the accuracy of the engine clutch torque estimation.

In conclusion, when comparing the estimators that combine the forward path and the backward path such as the model reference PI estimator and the Kalman filter based estimator with the forward path estimator in terms of actual vehicle application, the computation burden of the forward path estimator is smaller and the accuracy of the forward path estimator is similar to that of other estimators.

On the other hand, as for the limitations of the forward path estimator, as shown in Figs. 8 and 9, some amount of engine torque is generated during engine start-up before the clutch engages. However, as shown in Eq. (14), which is the filtering equation of the forward path estimator, the engine torque generated at this time should be canceled out with the engine inertia torque expressed by multiplication of the engine inertia and the derivative of the engine angular speed in the forward path estimator, and thus the estimated engine clutch torque should be the zero during engine start-up. However, in reality, as shown in Fig. 10, the engine torque that is generated during engine start-up before the clutch engages is not canceled out perfectly with the engine inertia torque due to the measurement error of the engine speed by sensor noise and resolution, as well as due to the unmodeled engine behavior, and thus the estimated engine clutch torque is not zero but fluctuates before the clutch is engaged.

Also, Fig. 12 shows the tendency that some of the estimated engine clutch torque by the forward path estimator within 8 to 13.5 mm of the piston position is larger than the zero. The clutch touch point is about 6.5 mm, and the fact that the piston position is between 8 and 13.5 mm means that the clutch is not touched yet. This would result from the measurement error of the engine speed by sensor noise and resolution, and the unmodeled engine behavior as well, as mentioned above.

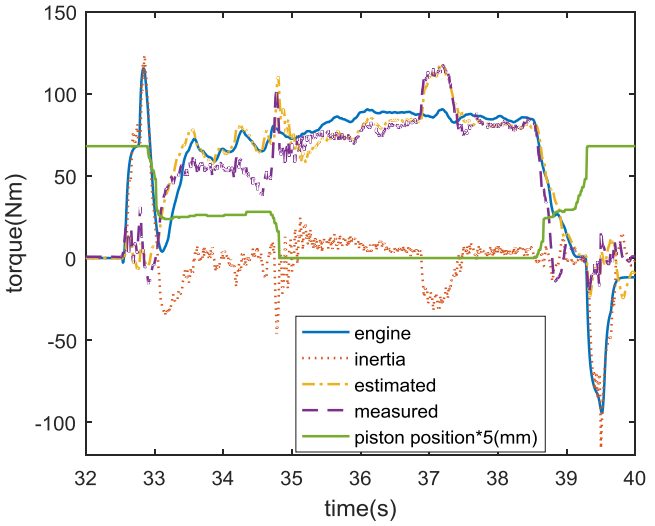

Fig. 13. Error analysis of the estimated engine clutch torque.

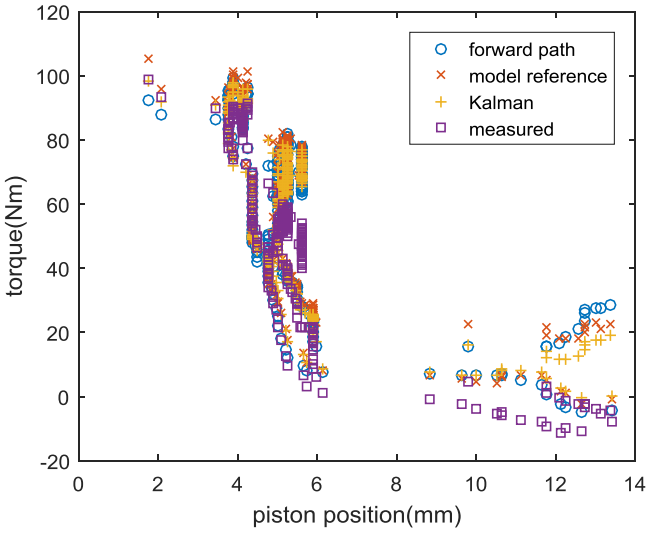

Fig. 14. Estimated T-S curve data during slipping phase of engine clutch.

In the same context, Fig. 12 also shows that some of the estimated torque by the forward path estimator within 3 to 7 mm of the piston position is larger than the measured torque. This would result from the engine torque error during the slipping engagement. This can be seen in Fig. 13. This figure shows the engine torque, the engine inertia torque expressed as the product of the engine inertia and the derivative of the engine angular speed, the estimated engine clutch torque by the forward path estimator, the measured engine clutch torque, and the piston position multiplied by the constant 5 during the experiment. In Fig. 13, it can be seen that there is some error between the estimated and the measured engine clutch torque in the section from 33.5 to 34.5 s. At this time, the inertia torque of the engine is close to zero, which indicates that the error of the estimated engine clutch torque results from the engine torque. This results shows that the engine torque estimation is important during a torque transient situation, and study of the engine torque estimation is left for future work.

Nevertheless, as shown in Figs. 10 and 11, the estimated T-S curve data show a similar tendency with the measured data within a piston position of 3 to 7 mm, and hence the estimated T-S curve data within 3 to 7 mm of the piston position were extracted and utilized for the adaptation of the friction model and the slip control of the engine clutch in a later experiment.

4.2. Clutch friction model adaptation and torque tracking control

In this subsection, the adaptation algorithm of the clutch friction model and the feedforward control method proposed in this paper were verified through another experiment with a production parallel hybrid vehicle.

During the second experiment, the engine clutch was slipping and engaged over ten times while the car started.

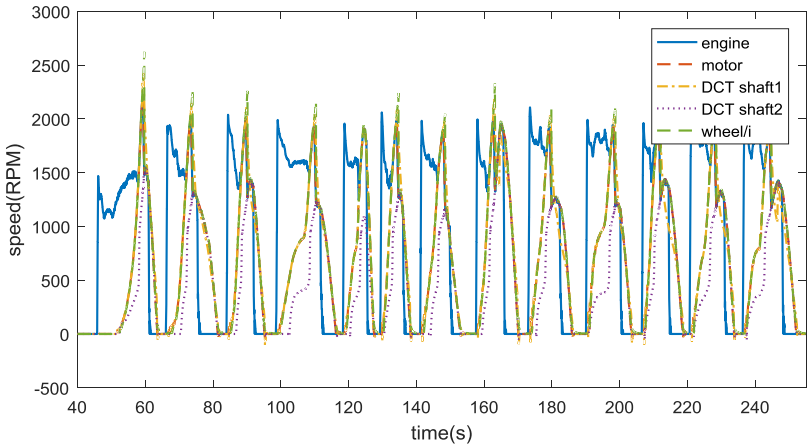

Fig. 15. Driveline speed during the verification experiment of the adaptation and control algorithm.

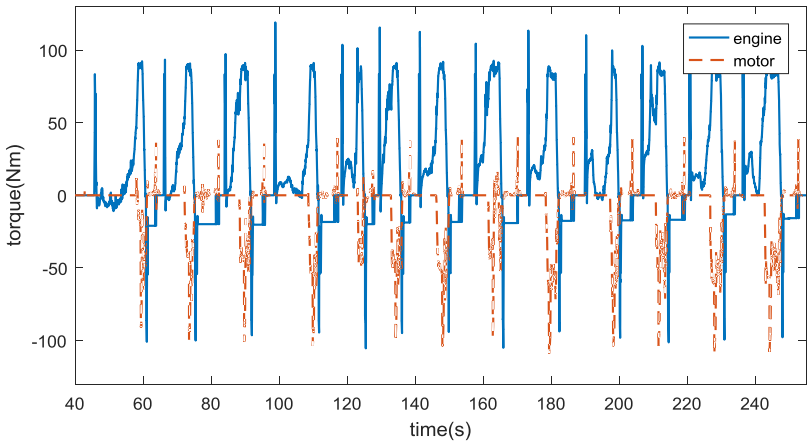

Fig. 16. Driveline torque during the verification experiment of the adaptation and control algorithm.

Table 3
RMS error of the target and estimated clutch torque during the adaptation period.

Time	RMS error (Nm)
First four engagements	29.04
Last four engagements	12.65

Figs. 15 and 16 show the driveline speed and torque during the verification experiment. In this experiment, the initial value of the friction coefficient gain and the clutch touch point were set as 2 and 6.57 mm, respectively, and the nominal clutch touch point was set as 6 mm. The friction coefficient gain and the clutch touch point were changed as shown in Fig. 17(a) and (b). Also, the amount of parallel drifting of the model was changed as presented in Fig. 17(c). As shown in Fig. 17(b) and (c), the clutch touch point moved up and down at around 6.5 mm, and the amount of variation of the clutch touch point was small since the actual touch point was not changed during the experiment. This shows that the adaptation of the clutch touch point was performed well during the experiment. Furthermore, as shown in Fig. 17(a), the friction coefficient gain converged to around 0.7 from the incorrect initial value of 2, and this shows that the adaptation of the friction coefficient gain was performed well.

Fig. 18 shows the target and estimated clutch torque during the experiment. In the second experiment, the clutch torque sensor was not installed in the experiment vehicle, and thus the estimated torque was considered as the actual torque. The similarity of the estimated and measured clutch torque was verified in the previous results section. In Fig. 18, the yellow line (dashdot) shows the adaptation period when the clutch slip speed and the clutch torque are larger than 20 rad/s and 0 Nm, respectively, and the piston position is between 3 and 7 mm and the engine clutch is being engaged.

Also, Table 3 shows the RMS error between the target and the estimated clutch torque in the first and last four engagements during the adaptation period. Fig. 18 shows that the clutch torque did not follow the target torque well in the

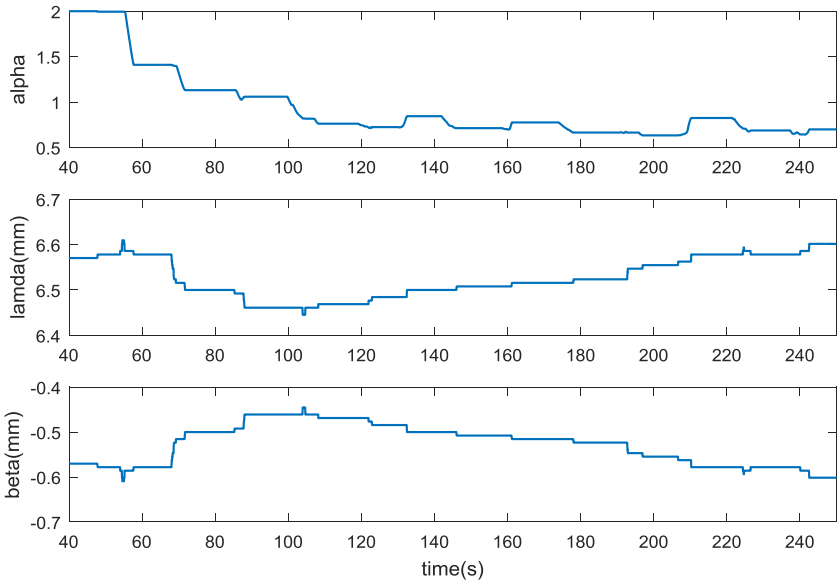

Fig. 17. Adaptation results during the verification experiment of the adaptation and control algorithm: (a) the estimated friction coefficient gain, (b) the estimated touch point, (c) the estimated amount of parallel drifting of the model.

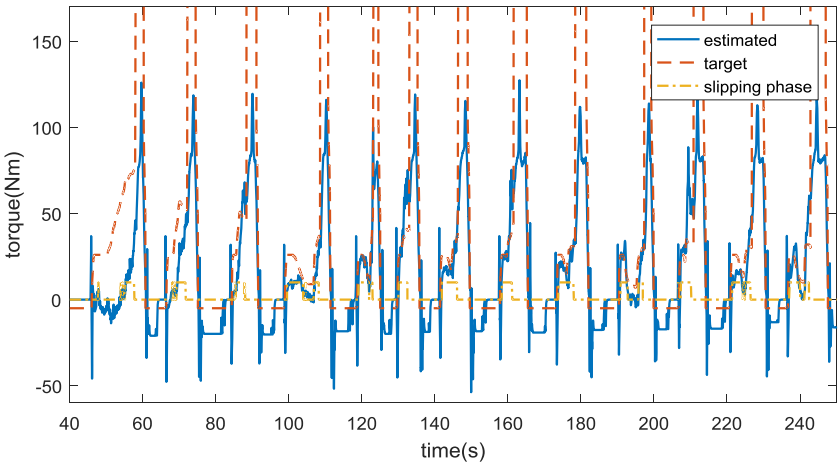

Fig. 18. Target and estimated clutch torque during the verification experiment of the adaptation and control algorithm.

beginning but the tracking performance became better over time while the friction coefficient gain and the amount of parallel drifting of the model were compensated. This table also shows that the torque tracking error decreased significantly due to the adaptation of the friction coefficient gain and the amount of parallel drifting of the model.

Furthermore, Fig. 19 shows the nominal T-S curve and the initial and compensated T-S curves. The initial and compensated models, where the friction coefficient gain and the amount of parallel drifting were applied, were utilized for the slip control.

5. Conclusion

This paper proposed a method for adaptive feedforward control of clutch torque during slip engagement of a dry clutch in a vehicle powertrain based on clutch torque estimation. The proposed method was applied to the slip engagement control of a dry engine clutch of a parallel hybrid vehicle, and was verified with production vehicle experiments. The engine clutch torque was first estimated using a driveline model. Furthermore, the clutch friction coefficient and the clutch touch point were estimated simultaneously to compensate the clutch friction model using the estimated engine clutch torque. The compensated clutch friction model was then utilized for feedforward control of the engine clutch during slip engagement. The clutch torque tracking performance was improved using the proposed algorithm and verified with production vehicle experiments. The experiments presented in this paper showed that the estimated clutch torque can be used to adapt a

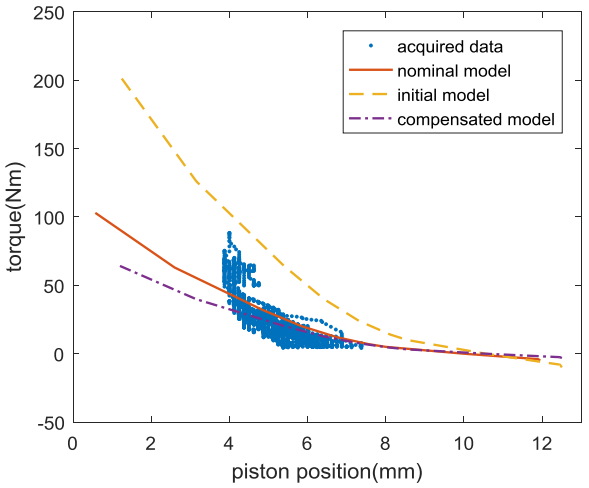

Fig. 19. Compensated clutch friction model during the verification experiment of the adaptation and control algorithm.

clutch friction model and control a clutch. For future work, a backward engine clutch torque estimator that can be utilized in a gradient road will be designed and the engine torque compensation method will be considered in order to improve the performance of the forward engine clutch torque estimator.

Acknowledgments

This research was partly supported by Hyundai Motor Company, a National Research Foundation of Korea (NRF) grant funded by the Korean government (MSIP) (No. 2017R1A2B4004116), and the BK21 + program through the NRF funded by the Ministry of Education of Korea.

Appendix

A. Model reference PI estimator of engine clutch torque

$$\dot{\hat{\omega}}_e = \frac{1}{J_e}T_e - \frac{1}{J_e}\hat{T}_{ec}$$

$$\dot{\hat{\omega}}_m = \frac{1}{J_m}\hat{T}_{ec} + \frac{1}{J_m}T_m - \frac{1}{J_m}\hat{T}_c$$

$$\dot{\hat{\omega}}_c = \frac{1}{J_c}\hat{T}_c - \frac{1}{J_c i_t i_f}\hat{T}_o$$

$$\dot{\hat{\omega}}_w = \frac{1}{J_v}\hat{T}_o - \frac{1}{J_v}\hat{T}_L$$

$$\hat{T}_{ec} = -L_{ecp}\dot{\tilde{\theta}}_{s1} - L_{eci}\tilde{\theta}_{s1}$$

$$\dot{\tilde{\theta}}_{s1} = (\omega_e - \omega_m) - (\hat{\omega}_e - \hat{\omega}_m)$$

$$\hat{T}_c = -L_{cp}\dot{\tilde{\theta}}_{s2} - L_{ci}\tilde{\theta}_{s2}$$

$$\dot{\tilde{\theta}}_{s2} = (\omega_m - \omega_c) - (\hat{\omega}_m - \hat{\omega}_c)$$

$$\hat{T}_o = k_o\left(\frac{\theta_c}{i_t i_f} - \theta_w\right) + b_o\left(\frac{\omega_c}{i_t i_f} - \omega_w\right) - L_{op}\dot{\tilde{\theta}}_{s3} - L_{oi}\tilde{\theta}_{s3}$$

$$\dot{\tilde{\theta}}_{s3} = (\omega_c - \omega_w) - (\hat{\omega}_c - \hat{\omega}_w)$$

$$\hat{T}_L = r_w \left\{ m_v g \sin(\theta_{road}) + K_{rr} m_v g \cos(\theta_{road}) + \frac{1}{2} \rho v_x^2 C_d A \right\} - L_{wp} \dot{\tilde{\theta}}_w - L_{wi} \tilde{\theta}_w$$

$$\dot{\tilde{\theta}}_w = \omega_w - \hat{\omega}_w$$

B. Kalman filter based estimator of engine clutch torque

$$\mathbf{F} = \mathbf{e}^{AT_s}, \mathbf{G} = \left(\int_0^{T_s} \mathbf{e}^{A\tau} \mathbf{d}\tau \right) \mathbf{B}, \mathbf{H} = \mathbf{C}$$

$$\mathbf{X}_k = \mathbf{F}\mathbf{X}_{k-1} + \mathbf{G}\mathbf{U}_{k-1}$$

$$\mathbf{Y}_k = \mathbf{H}\mathbf{X}_k$$

$$\hat{\mathbf{X}}_k^- = \mathbf{F}\hat{\mathbf{X}}_{k-1}^+ + \mathbf{G}\mathbf{U}_{k-1}$$

$$\mathbf{P}_k^- = \mathbf{F}\mathbf{P}_{k-1}^+ \mathbf{F}^T + \mathbf{Q}$$

$$\mathbf{K}_k = \mathbf{P}_k^- \mathbf{H}_k^T \left[\mathbf{H}_k \mathbf{P}_k^- \mathbf{H}_k^T + \mathbf{R} \right]^{-1}$$

$$\hat{\mathbf{X}}_k^+ = \hat{\mathbf{X}}_k^- + \mathbf{K}_k \left[\mathbf{Y}_k - \mathbf{H}\hat{\mathbf{X}}_k^- \right]$$

$$\mathbf{P}_k^+ = (\mathbf{I} - \mathbf{K}_k \mathbf{H}) \mathbf{P}_k^-$$

References

[1] K. van Berkel, F. Veldpaus, T. Hofman, et al., Fast and smooth clutch engagement control for a mechanical hybrid powertrain, IEEE Trans. Control Syst. Technol. 22 (2014) 1241–1254.
[2] M. Salman, N.J. Schouten, N.A. Kheir, Control strategies for parallel hybrid vehicles., in: Proceedings of the American Control Conference, IEEE, 2000, pp. 524–528.
[3] K.B. Wipke, M.R. Cuddy, S.D. Burch, ADVISOR 2.1: a user-friendly advanced powertrain simulation using a combined backward/forward approach, IEEE Trans. Veh. Technol. 48 (1999) 1751–1761.
[4] S. Kim, J. Oh, S. Choi, Gear shift control of a dual-clutch transmission using optimal control allocation, Mech. Mach. Theory 113 (2017) 109–125.
[5] T. Minowa, T. Ochi, H. Kuroiwa, et al., Smooth Gear Shift Control Technology For Clutch-To-Clutch Shifting, SAE Technical Paper, 1999 Report no. 0148-7191.
[6] G. Paganelli, T. Guerra, S. Delprat, et al., Simulation and assessment of power control strategies for a parallel hybrid car, Proc. Inst. Mech. Eng. Part D: J. Automob. Eng. 214 (2000) 705–717.
[7] H.-S. Jeong, K.-I. Lee, Friction coefficient, torque estimation, smooth shift control law for an automatic power transmission, KSME Int. J. 14 (2000) 508–517.
[8] H.-S. Jeong, K.-I. Lee, Shift characteristics analysis and smooth shift for an automatic power transmission, KSME Int. J. 14 (2000) 499–507.
[9] M. Kulkarni, T. Shim, Y. Zhang, Shift dynamics and control of dual-clutch transmissions, Mech. Mach. Theory 42 (2007) 168–182.
[10] C. Ni, T. Lu, J. Zhang, Gearshift control for dry dual-clutch transmissions, WSEAS Trans. Syst. 8 (2009) 1177–1186.
[11] J. Horn, J. Bamberger, P. Michau, et al., Flatness-based clutch control for automated manual transmissions, Control Eng. Pract. 11 (2003) 1353–1359.
[12] J. Kim, S.B. Choi, J. Oh, Adaptive engagement control of a self-energizing clutch actuator system based on robust position tracking, IEEE/ASME Trans. Mechatron. 23 (2018) 800–810.
[13] J.J. Oh, J.S. Eo, S.B. Choi, Torque observer-based control of self-energizing clutch actuator for dual clutch transmission, IEEE Trans. Control Syst. Technol. 25 (2017) 1856–1864.
[14] H. Kong, C. Zhang, H. Wang, et al., Engine clutch engagement control for a parallel hybrid electric vehicle using sliding mode control scheme, Aust. J. Electr. Electron. Eng. 13 (2016) 244–257.
[15] B.K. Shin, J.O. Hahn, K.I. Lee, Development of Shift Control Algorithm Using Estimated Turbine Torque, SAE Technical Paper, 2000 Report no. 0148-7191.
[16] L. Glielmo, L. Iannelli, V. Vacca, et al., Gearshift control for automated manual transmissions, IEEE/ASME Trans. Mech. 11 (2006) 17–26.
[17] J. Park, Development of engine clutch control for parallel hybrid vehicles., in: Proceedings of the World Electric Vehicle Symposium and Exhibition (EVS27), IEEE, 2013, pp. 1–5.
[18] A. Tarasow, C. Bohn, G. Wachsmuth, et al., Method for Identification of the Kiss Point as Well as Takeoff Point of a Hydraulically Actuated Friction Clutch, SAE Technical Paper, 2012 Report no. 0148-7191.
[19] J.J. Oh, S.B. Choi, Real-time estimation of transmitted torque on each clutch for ground vehicles with dual clutch transmission, IEEE/ASME Trans. Mechatron. 20 (2015) 24–36.
[20] J.J. Oh, S.B. Choi, J. Kim, Driveline modeling and estimation of individual clutch torque during gear shifts for dual clutch transmission, Mechatronics 24 (2014) 449–463.
[21] J. Oh, S. Choi, Y. Chang, et al., Engine clutch torque estimation for parallel-type hybrid electric vehicles, Int. J. Automot. Technol. 18 (2017) 125–135.

[22] S. Kim, S. Choi, Control-oriented modeling and torque estimations for vehicle driveline with dual-clutch transmission, Mech. Mach. Theory 121 (2018) 633–649.
[23] X. Zhu, F. Meng, H. Zhang, et al., Robust driveshaft torque observer design for stepped ratio transmission in electric vehicles, Neurocomputing 164 (2015) 262–271.
[24] P.A. Ioannou, J. Sun, Robust Adaptive Control, PTR Prentice-Hall, Upper Saddle River, NJ, 1996.
[25] S. Sastry, M. Bodson, Adaptive Control: Stability, Convergence and Robustness, Courier Corporation, 2011.
[26] B. Friedland, Y.-J. Park, On adaptive friction compensation, IEEE Trans. Autom. Control 37 (1992) 1609–1612.